Finite element simulation of three-dimensional particulate flows using mixture models

Yuliya Gorb[a], Otto Mierka[b], Liudmila Rivkind[c], Dmitri Kuzmin[d]

[a] *Department of Mathematics, University of Houston*
651 PGH, Houston, TX 77204-3008, USA
[b] *Institute of Applied Mathematics III, Dortmund University of Technology,*
Vogelpothsweg 87, D-44227, Dortmund, Germany
[c] *Institute of Applied Mathematics III, Dortmund University of Technology,*
Vogelpothsweg 87, D-44227, Dortmund, Germany
[d] *Institute of Applied Mathematics III, Dortmund University of Technology,*
Vogelpothsweg 87, D-44227, Dortmund, Germany

Abstract

In this paper, we discuss the numerical treatment of three-dimensional mixture models for (semi-)dilute and concentrated suspensions of particles in incompressible fluids. The generalized Navier-Stokes system and the continuity equation for the volume fraction of the disperse phase are discretized using an implicit high-resolution finite element scheme, and maximum principles are enforced using algebraic flux correction. To prevent the volume fractions from exceeding the maximum packing limit, a conservative overshoot limiter is applied to the converged convective fluxes at the end of each time step. A numerical study of the proposed approach is performed for 3D particulate flows over a backward-facing step and in a lid-driven cavity.

Keywords: particle-laden flows, mixture model, Boussinesq approximation, effective viscosity, finite elements, flux-corrected transport

Email addresses: gorb@math.uh.edu (Yuliya Gorb),
omierka@mathematik.uni-dortmund.de (Otto Mierka),
rivkind@mathematik.uni-dortmund.de (Liudmila Rivkind),
kuzmin@math.uni-dortmund.de (Dmitri Kuzmin)

1. Introduction

Flows of incompressible fluids carrying suspensions of rigid particles occur very commonly in science, nature, and technology. Due to the complexity of mechanisms that govern fluid-particle and particle-particle interactions, numerical simulation of such flows belongs to the most challenging problems in Computational Fluid Dynamics (CFD). The heterogeneous nature of disperse two-phase flows has engendered a hierarchy of models that cover the whole range of relevant scales and differ greatly in their complexity.

In this paper, we consider averaged continuum models in which the effective density and viscosity of the mixture depend on the local volume fraction of the disperse phase [12, 13]. In the dilute regime, we use an analog of the Boussinesq approximation for natural convection flows. The numerical implementation of the presented mixture model is based on the methodology we developed in [11] for buoyancy-driven turbulent bubbly flows.

When it comes to simulating dense suspensions, it is essential to ensure that the volume fraction of the disperse phase is bounded above. A typical model for dense suspensions incorporates an interparticle stress term designed to keep the particle volume fraction below the close-packing value [1, 6, 17]. Leiderman and Fogelson [15] multiplied the convective flux by a monotonically decreasing function of the volume fraction to impair the ability of particles to move into regions packed with other particles.

The flux-corrected transport (FCT) algorithm proposed in [10] combines the idea of Leiderman and Fogelson [15] with algebraic flux correction [9]. Instead of modifying the convective flux at the continuous level, we decompose the discretized convective term into numerical fluxes and limit the magnitude of these fluxes so as to get rid of unrealistic maxima. The advantages of constraining the discrete solution in this way are twofold. First, there is no need for tuning any free parameters or choosing the 'right' damping function for the convective flux. Second, the employed limiting strategy does not prevent the particles from leaving the regions of maximum concentration.

In the original publication [10], we applied the overshoot limiter to a 2D implosion problem with a prescribed velocity field. In the present paper, we use the same strategy to enforce the maximum principle for volume fractions in 3D mixture models of particulate flows. The numerical results for two test problems (backward-facing step and lid-driven cavity) illustrate the ability of the proposed scheme to handle dilute and concentrated suspensions.

2. Mixture model

In mixture models of disperse two-phase flows, the velocity $\mathbf{u}$ and pressure p of the suspension are given by the incompressible Navier-Stokes equations

$$\frac{\partial(\rho\mathbf{u})}{\partial t} + \nabla\cdot(\rho\mathbf{u}\otimes\mathbf{u}) = -\nabla p + \nabla\cdot(2\mu\mathcal{D}(\mathbf{u})) + \rho\mathbf{g}, \tag{1}$$

$$\nabla\cdot\mathbf{u} = 0, \tag{2}$$

where ρ is the effective density, $\mathcal{D}(\mathbf{u}) = \frac{1}{2}(\nabla\mathbf{u} + \nabla\mathbf{u}^T)$ is the strain rate tensor, μ is the effective viscosity, and $\mathbf{g}$ is the gravitational acceleration.

The hydrodynamic behavior of the mixture depends on the local volume fraction α of the disperse phase. In the fully Eulerian modeling framework, the evolution of α is governed by the hyperbolic continuity equation

$$\frac{\partial\alpha}{\partial t} + \nabla\cdot(\alpha\mathbf{u}_p) = 0, \tag{3}$$

where $\mathbf{u}_p$ is the average velocity of the particles. The average velocity of the fluid phase is denoted by $\mathbf{u}_f$. The relative velocity $\mathbf{u}_r = \mathbf{u}_p - \mathbf{u}_f$ is known as the slip velocity, settling velocity, or sedimentation velocity. It can be determined using empirical correlations (see below).

The effective density and momentum of the mixture are given by [5]

$$\rho = (1-\alpha)\rho_f + \alpha\rho_p, \tag{4}$$

$$\rho\mathbf{u} = (1-\alpha)\rho_f\mathbf{u}_f + \alpha\rho_p\mathbf{u}_p, \tag{5}$$

where ρ_p is the density of the solid and ρ_f is the density of the fluid. It follows that $\mathbf{u}_p$ can be expressed in terms of $\mathbf{u}$ and $\mathbf{u}_r$ as follows [12]:

$$\mathbf{u}_p = \mathbf{u} + \frac{1-\alpha}{1+\alpha\Theta}\mathbf{u}_r, \qquad \Theta = \frac{\rho_p}{\rho_f} - 1.$$

The model is closed by problem-dependent constitutive laws for $\mathbf{u}_r$ and μ.

3. Boussinesq approximation

In the dilute flow regime, the mixture behaves as a weakly compressible fluid and can be modeled using an analogy to the Boussinesq approximation for natural convection flows. The use of this approach in the context of disperse two-phase flow modeling goes back to the work of Lapin and Lübbert

[14] and Sokolichin et al. [18, 19]. As shown by Lalli [13], it is well suited for simulating dilute suspensions of particles in incompressible fluids.

Using $\rho \approx \rho_f$ in the left-hand side of the momentum equation (1) and the constant effective viscosity $\mu \approx \mu_f$ in the right-hand side, one obtains

$$\rho_f \left[\frac{\partial u}{\partial t} + \mathbf{u} \cdot \nabla \mathbf{u} \right] = -\nabla p + \mu_f \Delta \mathbf{u} + \rho_f \mathbf{g} + \alpha(\rho_p - \rho_f)\mathbf{g}.$$

Division by the constant density ρ_f yields the Boussinesq-like model [13]

$$\frac{\partial u}{\partial t} + \mathbf{u} \cdot \nabla \mathbf{u} = -\nabla \tilde{p} + \nu_f \Delta \mathbf{u} + \alpha \Theta \mathbf{g}, \tag{6}$$

$$\nabla \cdot \mathbf{u} = 0. \tag{7}$$

The kinematic viscosity ν_f and modified pressure $\tilde{p}$ are defined by

$$\nu_f = \frac{\mu_f}{\rho_f}, \qquad \nabla \tilde{p} = \frac{1}{\rho_f} \nabla p - \mathbf{g}.$$

The simplest constitutive relation for the relative velocity $\mathbf{u}_r$ is the Stokes law. For spherical particles of radius r_p, we have

$$\mathbf{u}_r = \frac{2}{9} \frac{r_p^2}{\nu_f} \Theta \mathbf{g}. \tag{8}$$

For more general closure approximations, we refer to the literature [4, 5, 7].

4. Effective viscosity models

In the Newtonian flow regime, the effective viscosity of a particle suspension depends on the volume fraction of the disperse phase but not on the shear rate. It can be calculated, e.g., using the constitutive equation [12]

$$\mu = \mu_f \left(1 + \frac{3}{2} \frac{\alpha}{1 - \frac{\alpha}{\alpha_M}} \right)^2, \tag{9}$$

where α_M is the maximum packing fraction and α_m is the critical value at which the viscoplastic behavior arises, see [12, 13] for details.

Another popular empirical formula was proposed by Krieger [8, 20]

$$\mu = \mu_f \left(1 - \frac{\alpha}{\alpha_M} \right)^{-\frac{5}{2}\alpha_M}. \tag{10}$$

In the case of high particle loads, the generalized Navier-Stokes system (1)–(2) should be solved instead of the simplified model (6)–(7). Moreover, the effective viscosity μ of a dense suspension depends not only on the volume fraction α but also on the second invariant of the strain rate tensor

$$\mathcal{D}_{II} = \sqrt{\frac{1}{2}\mathcal{D}(\mathbf{u}) : \mathcal{D}(\mathbf{u})}.$$

The rheology of a suspension that behaves as a Bingham fluid can be modeled using the constitutive equation proposed by Lalli et al. [12, 13]

$$\mu = \frac{\tau_0}{2}(\mathcal{D}_{II} + \epsilon)^{-1/2}. \tag{11}$$

The parameters of this model are the yield stress τ_0 and the regularization parameter ϵ which is used to control the magnitude of μ. Since the volume fraction of particles may be large in some subdomains and small in other subdomains, a combination of (11) with (9) or (10) may be employed.

Shear-induced particle migration can be taken into account by adding a diffusive flux $\mathbf{j} = -d_{\text{eff}}\nabla\alpha$ to the convective flux in (3). The effective diffusion coefficient can be determined using the model of Leighton and Acrivos [16]

$$d_{\text{eff}} = \alpha^2 r_p^2 \frac{\mathcal{D}_{II}}{3}\left(1 + \frac{e^{8.8\alpha}}{2}\right). \tag{12}$$

For a detailed presentation of existing models, we refer to [12, 13, 20].

5. Finite element discretization

The numerical implementation of the above models builds on the algorithm developed in [11] for numerical simulation of turbulent bubbly flows. The generalized Navier-Stokes system is solved using the multilevel Schur complement methods [22, 23] implemented in the parallel 3D version of the open-source finite element library FeatFlow [21]. The velocity and pressure are approximated using the stable Q_2P_1 pair on hexahedral meshes. The continuity equation (3) is discretized using Q_1 elements. The maximum principle for volume fractions is enforced using algebraic flux correction [9, 10]. The coupling with the Navier-Stokes solver is accomplished using outer iterations. Steady-state solutions are calculated using pseudo-time-stepping.

6. Overshoot limiter

It is worth mentioning that even the exact solution of the continuity equation (3) may exceed the maximum packing value α_M if the velocity $\mathbf{u}_p$ is not divergence-free. In order to enforce the physical maximum principle $\alpha \leq \alpha_M$, the convective flux must be set to zero in regions where the maximum concentration is attained. In this paper, we achieve this effect using the 3D version of the flux-corrected transport algorithm developed in [10].

In this section, we briefly describe the employed overshoot limiter. Given the maximum-packing bound α_M, we eliminate nonphysical maxima using the following flux-based representation of the discrete problem [10]

$$m_i \alpha_i^{n+1} = m_i \alpha_i^n + \Delta t \sum_{j \neq i} g_{ij}, \tag{13}$$

where m_i is a diagonal entry of the lumped mass matrix, Δt is the time step, and g_{ij} denotes a numerical flux from node j into node i.

In the process of algebraic flux correction, g_{ij} is multiplied by a solution-dependent correction factor $\beta_{ij} \in [0, 1]$. Since there are no undershoots, only positive fluxes require limiting. The algorithm for calculating β_{ij} becomes:

1. Compute the sums of positive convective fluxes into node i

$$P_i^+ = \sum_{j \neq i} \max\{0, g_{ij}\}. \tag{14}$$

2. Define the upper bounds for admissible increments

$$Q_i^+ = \frac{m_i}{\Delta t}(\alpha_M - \alpha_i^n). \tag{15}$$

3. Compute the nodal correction factors for the components of P_i^+

$$R_i^+ = \min\left\{1, \frac{Q_i^+}{P_i^+}\right\}. \tag{16}$$

4. Check the sign of the unconstrained flux and multiply g_{ij} by

$$\beta_{ij} = \begin{cases} R_i^+ & \text{if } g_{ij} > 0, \\ R_j^+ & \text{if } g_{ij} < 0. \end{cases} \tag{17}$$

This FCT-like limiter makes it possible to fix α^{n+1} with a single postprocessing step. However, the formula for β_{ij} is based on the worst-case scenario. Since positive fluxes are limited without knowing the magnitude of negative ones, unnecessary flux correction is performed if there is no overshoot at node i but the removal of negative fluxes would create an overshoot. This may lead to some erosion in regions where $\alpha^{n+1} \approx \alpha_M$. A possible remedy is iterative flux limiting. The contribution of negative fluxes can be taken into account using β_{ij} from the previous iteration to sharpen the bounds thus:

$$Q_i^+ = \frac{m_i}{\Delta t}(\alpha_M - \alpha_i^n) + \sum_{j \neq i} \beta_{ij} \min\{0, g_{ij}\}. \tag{18}$$

At the first iteration, we use $\beta_{ij} = 1$ so that the solution remains unchanged if the constraint $\alpha \leq \alpha_M$ is satisfied from the outset for all nodes.

7. Numerical examples

The following examples illustrate the ability of the proposed numerical algorithm to produce realistic results for particulate flow problems.

7.1. Backward-facing step

In the first example, we use the Boussinesq mixture model to simulate dilute particulate flow over a three-dimensional backward-facing step. The 2D prototype of this benchmark problem was introduced by Barton [2] who used an Euler-Lagrange flow model of the disperse two-phase flow. In the 3D version, we extrude the quadrilateral mesh shown in Fig. 1 into the third dimension and successively refine it to generate the hierarchical data structures for the geometric multigrid methods implemented in FeatFlow. In order to resolve the steep gradients in the boundary layer, we use anisotropic mesh refinement in the near-wall region on the coarse mesh.

In the first example, we simulate a dilute suspension using the Boussinesq model (6)-(7) with $\mu_f = 0.005$ and the Stokes law (8) for the sedimentation velocity. The densities of the two phases are given by $\rho_p = 10$ and $\rho_f = 1$, which corresponds to $\Theta = 9.0$. The value of the gravitational constant is $g = 0.3$ in this test. At the inlet, we prescribe a parabolic velocity profile with the mean velocity $v_{\text{in}} = 1$. The inflow boundary condition for the volume fraction of the disperse phase is given by $\alpha_{\text{in}} = 0.003$. On the solid walls, we prescribe the symmetry (free-slip) condition. At the outlet, we use the standard do-nothing condition for the effective stress of the mixture.

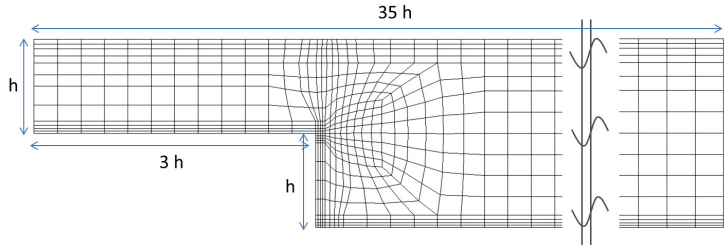

Figure 1: Computational coarse mesh.

The flow pattern is characterized by the Reynolds and Stokes numbers

$$\mathrm{Re} = \frac{v_{\mathrm{in}}(2h)\rho_f}{\mu_f} = 400, \qquad \mathrm{Stk} = \frac{2}{9}\frac{v_{\mathrm{in}} r_p^2}{(2h)}\frac{\rho_p}{\mu_f}.$$

The quasi-stationary distributions of the volume fraction α for $\mathrm{Stk} = 0.001$ and $\mathrm{Stk} = 0.01$ are displayed in Figs. 2 and 3. These solutions are in a good qualitative agreement with the results of the 2D simulation in [2].

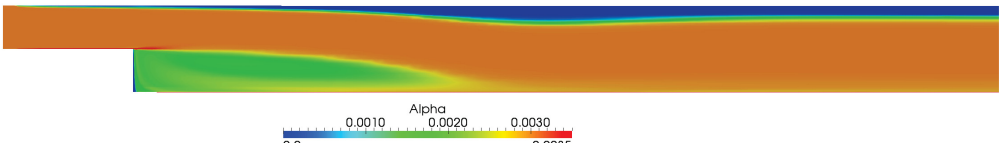

Figure 2: Backward-facing step: distribution of α in the plane $z = 0$ for $\mathrm{Stk} = 0.001$.

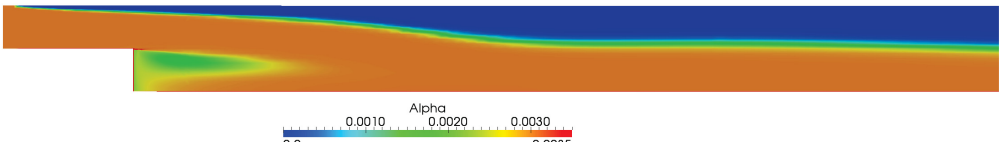

Figure 3: Backward-facing step: distribution of α in the plane $z = 0$ for $\mathrm{Stk} = 0.01$.

7.2. Lid-driven cavity

In the second example, we simulate the flow in a particle-laden lid-driven cavity using the 3D mixture model with the following parameter settings:

$$\Theta = 0.1, \qquad g = 0.1, \quad \rho_f = 1.0, \quad \mu_f = 0.01,$$

$$r_p = 0.001, \quad \tau_0 = 5.0, \quad \epsilon = 0.1.$$

The bound for α is given by the close random packing fraction $\alpha_M = 0.65$.

In this numerical study, we neglect the shear-induced mixing and calculate the effective viscosity μ using the following version of Krieger's model:

$$\mu = \mu_f \left(1 - \frac{\alpha}{\alpha_\infty}\right)^{-\frac{5}{2}\alpha_\infty}, \qquad 0 \le \alpha \le \alpha_M, \tag{19}$$

where $\alpha_\infty = 0.75$ is the void fraction for the maximum regular packing.

The domain $\Omega = (0,1) \times (0,1) \times (-0.1, 0.1)$ is discretized using 262,144 hexahedral elements. The Dirichlet boundary condition for the mixture velocity is given by $\mathbf{u} = (1,0,0)$ on the upper wall of the cavity, symmetry condition for $z = \pm 0.1$ and the no-slip condition $\mathbf{u} = (0,0,0)$ elsewhere.

The initial condition for the volume fraction α is given by

$$\alpha_0(x,y,z) = \begin{cases} \alpha_M, & \text{if } y \le 0.75 \\ 0, & \text{otherwise.} \end{cases}$$

The snapshots in Figs. 4 and 5 demonstrate the evolution of α and μ. Note that the changes in the distribution of α are reflected in the distribution of μ. The total volume of particles remains constant and the local volume fraction satisfies the maximum principle $0 \le \alpha \le \alpha_M$. This example shows the potential of our algebraic approach [10] to constraining the volume fractions in finite element simulation software for disperse two-phase flows.

8. Conclusions

The mixture models considered in this paper are well-suited for coarse-grained 3D simulations of particulate flows. The ability of these models to describe real-life physical phenomena relies on the validity of the underlying constitutive relations. In the presence of fine-scale effects that cannot be captured using the above closures, a more accurate estimate of the effective viscosity can be obtained, e.g., using a Lagrangian particle-scale model or the discrete network approximation [3]. We envisage that the use of adaptive model refinement will make it possible to develop advanced multiscale simulation tools for disperse two-phase flows. This task will also require further work on the design of numerical upscaling and downscaling methods.

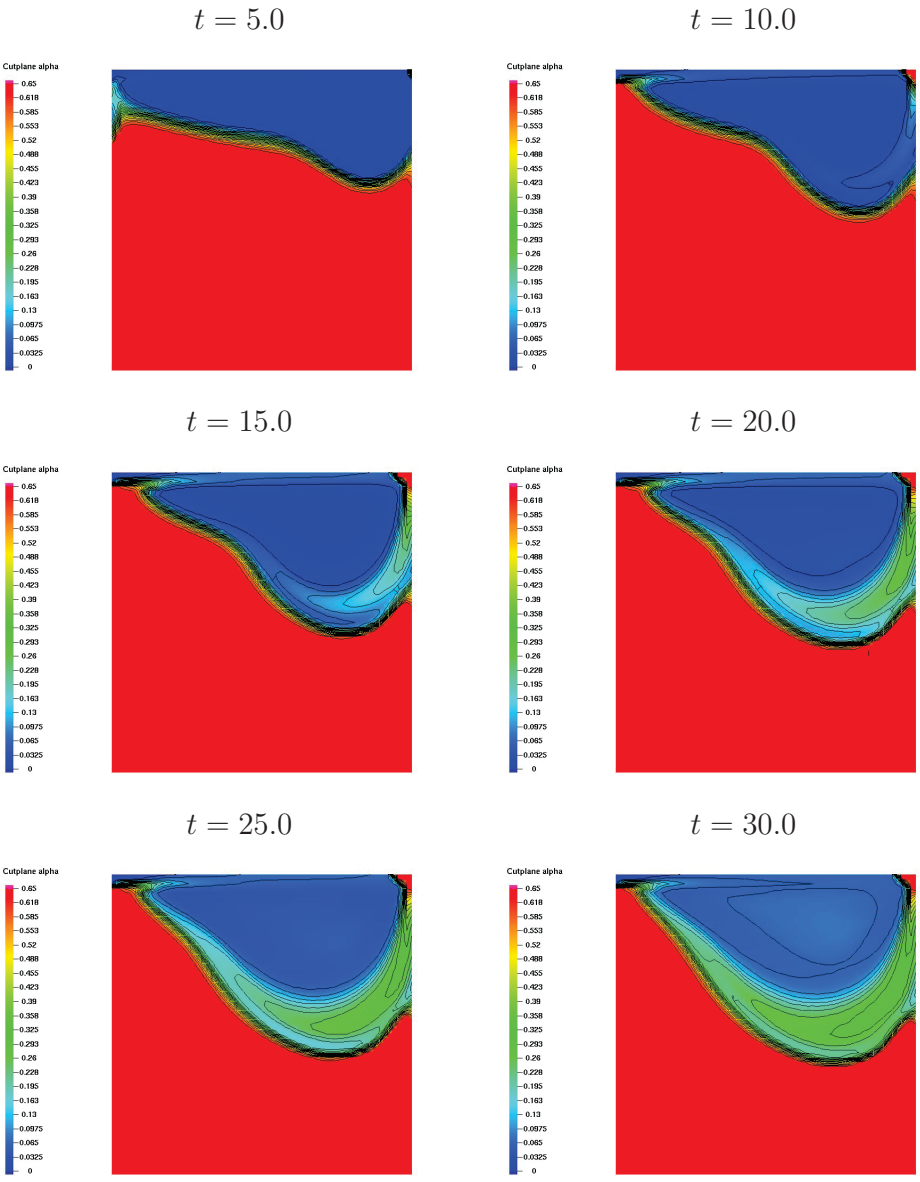

Figure 4: Lid-driven cavity: evolution of α in the plane $z = 0$.

Acknowledgments

The work of the first author was supported by the National Science Foundation under grant DMS-1016531. The research done at the Dortmund Uni-

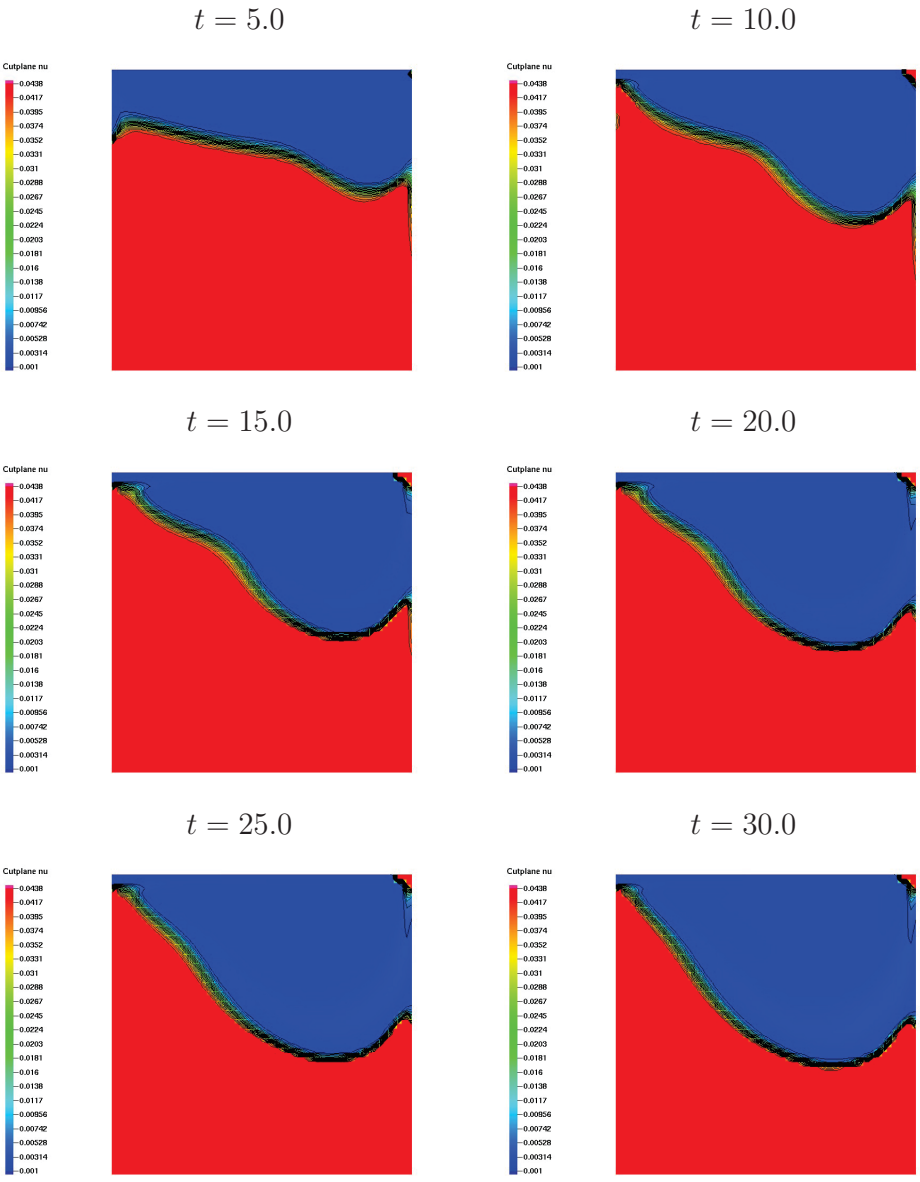

Figure 5: Lid-driven cavity: evolution of μ in the plane $z = 0$.

versity of Technology was sponsored by SFB 708 (3D Surface Engineering of Metal Sheet Manufacturing Equipment), a Collaborative Research Center funded by the German Research Association DFG.

References

[1] M. J. Andrews and P.J. O'Rourke, The multiphase particle-in-cell (MP-PIC) method for dense particulate flows. *Int. J. Multiphase Flow* **22** (1996) 379-402.

[2] I.E. Barton, Computation of dilute particular laminar flow over a backward-facing step. *Int. J. Numer. Methods Fluids* **22** (1996) 211-221.

[3] L. Berlyand, Y. Gorb, A. Novikov, Fictitious fluid approach and anomalous blow-up of the dissipation rate in a two-dimensional model of concentrated suspensions. *Arch. Ration. Mech. Anal.* **193** (2009) 585–622.

[4] D. Brennan, *The Numerical Simulation of Two-Phase Flows in Settling Tanks*, Ph.D. thesis, University of London, 2011.

[5] D.A. Drew and S.L. Passman, *Theory of Multicomponent Fluids*. Springer, 1999.

[6] D. Gidaspow, *Multiphase Flow and Fluidization: Continuum and Kinetic Theory Descriptions*. Academic Press, Boston, MA, 1994.

[7] K. Hiltunen, A. Jäsberg, S. Kallio, H. Karema, M. Kataja, A. Koponen, M. Manninen and V. Taivassalo, *Multiphase Flow Dynamics. Theory and Numerics.* VTT Publications **722** (2009).

[8] I.M. Krieger, Rheology of monodisperse latices. *Adv. Colloid Interface Sci.* **3** (1972) 111–136.

[9] D. Kuzmin, Algebraic flux correction I. Scalar conservation laws. In: D. Kuzmin, R. Löhner and S. Turek (eds.) *Flux-Corrected Transport: Principles, Algorithms, and Applications*. Springer: Scientific Computation, 2nd edition, 2012, pp. 145–192.

[10] D. Kuzmin and Y. Gorb, A flux-corrected transport algorithm for handling the close-packing limit in dense suspensions. *J. Comput. Appl. Math.* **236** (2012) 4944–4951.

[11] D. Kuzmin and S. Turek, Numerical simulation of turbulent bubbly flows. In: G.P. Celata, P. Di Marco, A. Mariani, R.K. Shah (eds) *Two-Phase Flow Modeling and Experimentation*. Edizioni ETS, Pisa, 2004, Vol. I, 179-188.

[12] F. Lalli, P.G. Esposito, R. Piscopia and R. Verzicco, Fluid-particle flow simulation by averaged continuous model. *Computers & Fluids* **34** (2005) 10401061.

[13] F. Lalli, P.G. Esposito and R. Verzicco, A constitutive equation for fluid-particle flow simulation. *Int. J. Offshore and Polar Engrg.* **16** (2006) 18-24.

[14] A. Lapin and A. Lübbert, Numerical simulation of the dynamics of two-phase gas-liquid flows in bubble columns. *Chem. Eng. Sci.* **49** (1994) 3661–3674.

[15] K. Leiderman and A.L. Fogelson, Grow with the flow: a spatial–temporal model of platelet deposition and blood coagulation under flow. *Math. Med. Biol.* **28** (2011) 47–84.

[16] D. Leighton and A. Acrivos, The shear-induced migration of particles in concentrated suspensions. *J. Fluid Mech.* **187** (1987) 415–439.

[17] N.A. Patankar and D.D. Joseph, Modeling and numerical simulation of particulate flows by the Eulerian-Lagrangian approach. *Int. J. Multiphase Flow* **27** (2001) 1659–1684.

[18] A. Sokolichin, *Mathematische Modellbildung und numerische Simulation von Gas-Flüssigkeits-Blasenströmungen*. Habilitation thesis, University of Stuttgart, 2004.

[19] A. Sokolichin, G. Eigenberger and A. Lapin, Simulation of buoyancy driven bubbly flow: established simplifications and open questions. *AIChE Journal* **50** (2004) no. 1, 24–45.

[20] J.J. Stickel and R.L. Powell, Fluid mechanics and rheology of dense suspensions. *Annu. Rev. Fluid Mech.* **37** (2005) 129–149.

[21] S. Turek et al., *FEATFLOW: finite element software for the incompressible Navier-Stokes equations.* User manual, University of Dortmund, 2000, `http://www.featflow.de`.

[22] S. Turek, *Efficient Solvers for Incompressible Flow Problems: An Algorithmic and Computational Approach*, LNCSE 6, Springer, 1999.

[23] S. Turek and D. Kuzmin, Algebraic flux correction III. Incompressible flow problems. In: D. Kuzmin, R. Löhner and S. Turek (eds.) *Flux-Corrected Transport: Principles, Algorithms, and Applications*. Springer: Scientific Computation, 2nd edition, 2012, pp. 239–298.